Molecular Human Reproduction, Vol.25, No.11, pp. 695–705, 2019
Advance Access Publication on October 2, 2019 doi:10.1093/molehr/gaz055

molecular human reproduction

ORIGINAL RESEARCH

The spatio-temporal dynamics of mitochondrial membrane potential during oocyte maturation

Usama AL-Zubaidi[1,2], Jun Liu[1], Ozgur Cinar[1,3], Rebecca L Robker[1,4], Deepak Adhikari[1,*], and John Carroll[1]

[1]Development and Stem Cell Program and Department of Anatomy and Developmental Biology, Monash Biomedicine Discovery Institute, Monash University, Melbourne, Victoria 3800, Australia [2]Applied Embryology Department, High Institute for Infertility Diagnosis and Assisted Reproductive Technologies, AL-Nahrain University, Baghdad, Iraq [3]Department of Histology and Embryology, Ankara University School of Medicine, Ankara, Turkey [4]School of Pediatrics and Reproductive Health, Robinson Research Institute, The University of Adelaide, Adelaide, SA, 5005, Australia

*Correspondence address. Development and Stem Cell Program and Department of Anatomy and Developmental Biology, Monash Biomedicine Discovery Institute, Monash University, Melbourne, Victoria 3800, Australia. E-mail: deepak.adhikari@monash.edu orcid.org/0000-0002-3404-8753

Submitted on May 3, 2019; resubmitted on September 3, 2019; editorial decision on September 13, 2019

ABSTRACT: Mitochondria are highly dynamic organelles and their distribution, structure and activity affect a wide range of cellular functions. Mitochondrial membrane potential ($\Delta\Psi m$) is an indicator of mitochondrial activity and plays a major role in ATP production, redox balance, signaling and metabolism. Despite the absolute reliance of oocyte and early embryo development on mitochondrial function, there is little known about the spatial and temporal aspects of $\Delta\Psi m$ during oocyte maturation. The one exception is that previous findings using a $\Delta\Psi m$ indicator, JC-1, report that mitochondria in the cortex show a preferentially increased $\Delta\Psi m$, relative to the rest of the cytoplasm. Using live-cell imaging and a new ratiometric approach for measuring $\Delta\Psi m$ in mouse oocytes, we find that $\Delta\Psi m$ increases through the time course of oocyte maturation and that mitochondria in the vicinity of the first meiotic spindle show an increase in $\Delta\Psi m$, compared to other regions of the cytoplasm. We find no evidence for an elevated $\Delta\Psi m$ in the oocyte cortex. These findings suggest that mitochondrial activity is adaptive and responsive to the events of oocyte maturation at both a global and local level. In conclusion, we have provided a new approach to reliably measure $\Delta\Psi m$ that has shed new light onto the spatio-temporal regulation of mitochondrial function in oocytes and early embryos.

Key words: oocyte maturation / mitochondria / membrane potential / JC-1 / TMRM

Introduction

Mitochondria regulate a number of cellular functions including ATP production, metabolism, Ca^{2+} homeostasis and cell death. Mitochondrial functions are primarily driven as a result of the bioenergetic properties of the electron transport chain, which pumps hydrogen ions across the inner mitochondrial membrane creating a highly negative mitochondrial membrane potential ($\Delta\Psi m$). To generate ATP, hydrogen ions move back down this electrochemical gradient driving the ATP synthase in the process (Mitchell and Moyle, 1967). Mitochondrial ATP production is particularly critical in oocytes and early mammalian embryos because there is a block to glycolysis that is only relieved at the morula-blastocyst transition (reviewed in Grindler and Moley, 2013). The absolute reliance of oocytes and preimplantation embryos on mitochondrial ATP production has led to a significant focus on the role and function of mitochondria in the developmental potential of oocytes and early embryos (Eichenlaub-Ritter *et al.*, 2004; Zhang *et al.*, 2006; Wang *et al.*, 2009; Ben-Meir *et al.*, 2015; Boots *et al.*, 2016).

Oocyte developmental competence and ability to support embryonic development are often linked with the mitochondria-dependent bioenergetic capacity (reviewed in Grindler and Moley, 2013). Interventions that inhibit mitochondrial function cause defects in meiotic and mitotic spindles and inhibit oocyte maturation and embryo development (Zhang *et al.*, 2006; Dalton *et al.*, 2014; Wu *et al.*, 2015). Furthermore, environmental or pathophysiological challenges including obesity, metabolic disease, maternal ageing and oxidative stress are all associated with defects in oocyte mitochondria such as altered $\Delta\Psi m$, localization, altered cristae structure and reduced ATP production (Ottosen *et al.*, 2007; Grindler and Moley, 2013; Tilly and Sinclair, 2013; Wu *et al.*, 2015; Pasquariello *et al.*, 2019). These functional effects are correlated with poor developmental outcomes in embryos, which place mitochondrial activity as a major determinant of oocyte quality or competence.

During in vitro oocyte maturation, there is a dramatic redistribution of mitochondria. In germinal vesicle (GV) stage mouse oocytes, they are relatively homogeneously distributed but after germinal vesicle

breakdown (GVBD) and as the metaphase I spindle forms mitochondria aggregate with the endoplasmic reticulum (ER) around the developing first meiotic spindle (Van Blerkom and Runner, 1984; Dalton and Carroll, 2013). This is an active process dependent on dynein-mediated trafficking on microtubules. The cytoplasmic superstructure comprising the metaphase I (MI) spindle enveloped in a sheath of ER and mitochondria is then moved via actin-mediated forces to the cortex (Dalton and Carroll, 2013) where anaphase is initiated and the first polar body is extruded. Mitochondria then redistribute around the cytoplasm in preparation for fertilization at metaphase II (MII). These changes in mitochondrial distribution correlate with increased ATP levels during spindle formation and at polar body formation (Yu *et al.*, 2010; Dalton and Carroll, 2013; Dalton *et al.*, 2014), suggesting that mitochondrial activity may adapt to metabolic demand.

Mitochondrial membrane potential can be measured using a number of potentiometric cationic fluorescent indicators such as tetraethylbenzimidazolylcarbocyanine iodide (JC-1), tetramethylrhodamine methyl ester (TMRM) and Rhod-2. Through the use of JC-1 in oocytes and embryos, it has long been reported and has become widely accepted that $\Delta\Psi m$ is spatially organized such that mitochondria in the cortex have a higher $\Delta\Psi m$ relative to those in the peri-nuclear region (Van Blerkom *et al.*, 2000; Van Blerkom *et al.*, 2008; Tatone *et al.*, 2011; Zhao *et al.*, 2011; Boudoures *et al.*, 2017; Pasquariello *et al.*, 2019). This reported high cortical $\Delta\Psi m$ has implications for understanding the role of mitochondria in oocytes and embryos. For example, the high cortical $\Delta\Psi m$ has been purported to be important for Ca^{2+} handling at fertilization, while the low $\Delta\Psi m$ deeper in the cytoplasm implies that low levels of mitochondrial activity are sufficient to drive the events of spindle formation and function (Van Blerkom and Davis, 2007).

It is of interest that the highly polarized mitochondria in the cortex are reported in all studies using JC-1 but not in those that utilize TMRM (or other single wavelength indicators). JC-1 is lipophilic and cationic, which allows its accumulation in mitochondria. It has complex spectral properties such that at low concentrations, it is monomeric and emits in the green, while at high concentrations, there is a spectral shift to red emission because of so called 'J-aggregate' formation. As such, the red:green emission ratio gives a relative measure of $\Delta\Psi m$ in the cell. The highly polarized cortical mitochondria indicated by JC-1 are not seen in studies using single wavelength indicators such as TMRM (Dumollard *et al.*, 2004, Zhang *et al.*, 2006, Igosheva *et al.*, 2010). TMRM is a small cationic fluorescent indicator that accumulates in mitochondria purely based on $\Delta\Psi m$. These contrasting observations arising from different laboratories using different indicators suggests the need to revisit the question as to whether there is a spatial heterogeneity in $\Delta\Psi m$ in oocytes and embryos.

The increasing appreciation of mitochondrial function in oocytes and the potential for using mitochondrial activators, or mitochondrial supplementation/donation for improving oocyte quality or avoiding mitochondrial genetic disease, makes it an imperative that accurate and reliable methods are available for measuring mitochondrial function. In this study, we have validated a novel ratiometric approach to measure $\Delta\Psi m$ in oocytes and embryos. We use the assay to measure $\Delta\Psi m$ through the time course of oocyte maturation and reveal for the first time $\Delta\Psi m$ heterogeneity in sub-cellular compartments, most notably in the mitochondria surrounding the MI spindle. Our measurements of $\Delta\Psi m$ using these approaches show no evidence for polarized cortical mitochondria.

Materials and Methods

Oocyte collection

Oocytes at the GV stage were collected from 3- to 4-week-old C57 female mice. These mice had been stimulated by intraperitoneal injection of 7 international units (IU) pregnant mare's serum gonadotropin (PMSG; Intervet, Buckinghamshire, UK) 44–48 hours prior to oocyte retrieval. After removing adipose tissue surrounding the ovaries, cumulus oocyte complex (COC) containing fully grown GV-stage oocytes encircled by cumulus cells was released by puncturing the ovaries in M2 medium supplemented with 200 μM 3-isobutyl-1-methylxanthine (IBMX) (Sigma-Aldrich, St. Louis, Missouri, USA) to maintain GV arrest at 37°C. Attached cumulus cells were removed by repetitive pipetting of COCs. *PhAM*$^{loxP/loxP}$ mice (Jax mice stock no: 018385) (Pham *et al.*, 2012) were crossed with transgenic mice that carried *Gdf-9* promoter-mediated Cre recombinase, which had a C57BL/6J background (Lan *et al.*, 2004). Homozygous mutant female mice expressed a mitochondrial-specific version of Dendra2 green/red photo switchable monomeric fluorescent protein exclusively in oocytes (*PhAM*$^{loxP/loxP}$; *Gdf9-Cre*). All mice were housed under controlled environmental conditions with free access to water and food. The Animal Ethics Committee of Monash University approved all animal handling and experimental protocols.

IVF and embryo culture

For in vitro fertilization, female mice (3–4 week) were primed with 5 IU PMSG and 5 IU human chorionic gonadotropin (hCG). One night before fertilization, human tubal fluid (HTF, Merck Millipore, Billerica, Massachusetts, USA) drops (50 μl/drop) and culture medium (CM, Life Global group, Belgium) overlaid with mineral oil (Sigma) were equilibrated in an incubator at 37°C and 5% CO_2 in air. One hour before oocyte collection, sperm were collected from cauda epididymides of 12-week-old C57 males into 1-ml HTF and placed in CO_2 incubator for capacitation. The COCs were mixed with capacitated sperm HTF drops and incubated for 2–4 hours. COCs were then washed through CM drops three times and were cultured in CM medium and monitored for the appropriate time to obtain 2-cell and 4-cell embryos.

Use of probes and inhibitors

All probes were loaded in drops of M2 under oil at 37°C. The concentration and loading times are provided in the relevant figure legends. In short, three different concentrations of JC-1 (0.5, 1 and 5 μg ml^{-1}), 25 nM of TMRM, and 100 nM of MitoTracker Green (MTG) were used to visualize mitochondria. In some experiments requiring dynamic time-lapse measurement of mitochondrial membrane potential, a low concentration of TMRM (5 nM) was included in the imaging drops. FCCP (Carbonyl cyanide-4-(trifluoromethoxy)phenylhydrazone) (0.5, 1 and 5 μM) was added directly to the imaging drops between acquisitions.

Confocal microscopy

Live-cell imaging was performed on an inverted confocal microscope (SP8, Leica, Germany) fitted with an environmentally controlled

chamber to maintain a temperature of 37°C. Oocytes loaded with mitochondrially targeted probes, JC-1 (Sigma), TMRM (Sigma) and MTG (Thermo Fisher, Waltham, Massachusetts, USA) were placed in drops of M2 in an imaging chamber with a coverslip as its base. Images were acquired using a 40× water immersion 1.2 *N A* objective with line averaging set to 2–4. It should be noted that on exposure to UV, Dendra can be photoconverted to red emission wavelengths. We confirmed that using the excitation conditions in our experiments, Dendra did not undergo any photoconversion and was therefore suitable as a reliable and stable reporter of mitochondrial mass.

Ratiometric image analysis

Ratiometric analysis was performed using ImageJ software (NIH). Briefly, Dendra (green) and TMRM (red) channels of the confocal images were separated and converted to 32-bit images, and the background of each channel was set to not a number using thresholding. The thresholded TMRM fluorescence images were then divided by the Dendra fluorescence image pixel by pixel using the Image Calculation function in ImageJ software.

Experimental design and statistical analysis

Experiments were repeated at least three times and number of oocytes/embryos was taken as *n* for statistical analyses and mean and SD (or SEM) were calculated. Oocyte/embryos from 1–2 mice were used for each repeat. Error bars indicate SD or SE of the mean as mentioned in the individual results. Statistical analysis was performed using either student t-test or one-way ANOVA with Microsoft Excel or GraphPad Prism Software. Level of significance is denoted by $^{*}P < 0.05$, $^{**}P < 0.01$, $^{***}P < 0.001$ and $^{****}P < 0.0001$ as shown in the figures.

Results

Monitoring spatial distribution of $\Delta\Psi$m with JC-1 and TMRM

The two most common approaches for monitoring $\Delta\Psi$m are through the use of either JC-1 or TMRM. Loading of mouse GV stage oocytes with JC-1 (1.0 μg/ml) for 30 minutes prior to imaging using confocal microscopy confirmed published observations that there was a bright cortical ring of red J-aggregate fluorescence and very low levels deeper in the cytoplasm (Fig. 1A, i), while the monomer appeared relatively evenly distributed across the cytoplasm (Fig. 1A, ii). The J-aggregate (red)/monomer (green) ratio was therefore much higher in the cortex than in the deeper cytoplasm, indicating, at face value, that $\Delta\Psi$m is significantly elevated in the cortex.

We next measured the cortical/cytoplasmic distribution of the J-aggregate and monomer, finding an approximate 8-fold accumulation of J-aggregate in the cortex (Fig. 1C). In contrast, the monomer was more evenly distributed with a ratio closer to 2 (Fig. 1C). To explore the spatial distribution of J-aggregate further and investigate the relevance to $\Delta\Psi$m, oocytes were loaded with the potentiometric indicator TMRM (25 nM for 30 minutes). In contrast to JC-1, no obvious gradient of fluorescence intensity was evident and this was reflected in a cortex/cytoplasm ratio that was consistently very close to unity (Fig. 1B and C). To examine if this difference between JC-1 and TMRM behaviors is specific to GV stage oocytes, we performed similar measurements in two-cell (Fig. 1D–F) and four-cell embryos (Fig. 1G–I). At both stages of development, the J-aggregate distribution ratio was greater than 5 while that of TMRM was consistently at unity (Fig. 1F and I).

JC-1 distribution is highly concentration- and time dependent

By varying the loading dose of JC-1, we found that the J-aggregate cortex/cytoplasm ratio was highly concentration dependent; but even concentrations as low as 0.5 μg/ml maintained a J-aggregate ratio of approximately 7 (Fig. 2A and B and Fig. S1). Since lower concentrations were not compatible with a reliable fluorescence signal, we next increased loading times to determine if an increased equilibration time could lead to a normalized distribution of J-aggregates. There was a strong inverse correlation between the J-aggregate cortical/cytoplasmic ratio and time, with a ratio of 8.19 ± 0.71 for a 30-minute loading decreasing to 3.42 ± 0.66 over a 2-hour loading period (Fig. 2C and D and Fig. S1). Furthermore, this was similar if the loading period was confined to 30 minutes and then followed by a prolonged equilibration period in JC-1-free medium (Fig. S2A and B). It is unclear if J-aggregate distribution would eventually reach equilibration with even longer loading times, but the potential deleterious impact of prolonged exposure to JC-1 may then bring into question the reliability and practicality in an experimental setting. This conclusion is supported by the finding that 2-cell embryos loaded with JC-1 (30 minutes; 1.0 μg/ml) failed to progress to the 4-cell stage and started to degenerate (Fig. S3 D and E); while after loading with TMRM, over 80% progressed to the 4-cell stage (Fig. S3 A, B and E). Taken together, these data demonstrate that JC-1 distribution is influenced by concentration and equilibration time and that these need to be balanced against potential toxicity.

TMRM and JC-1 can reliably report dynamic changes in $\Delta\Psi$m in oocytes

The data presented to date suggest that the properties of J-aggregates to preferentially accumulate in the cortex may make JC-1 an unreliable indicator for the spatial distribution of $\Delta\Psi$m in oocytes and embryos. Nevertheless, it may remain valid for the measurement of $\Delta\Psi$m at the whole-cell level. Oocytes were loaded with JC-1 (30 minutes; 1.0 μg/ml) and fluorescence was recorded using confocal microscopy. On application of FCCP, the J-aggregate signal decreased while the monomer signal increased (Fig. S4A), confirming that on depolarization of $\Delta\Psi$m, J-aggregates revert to monomers and the ratio of both wavelengths can be plotted to obtain a time course of mitochondrial membrane potential collapse (Fig. S4B). As expected, TMRM, which localizes to mitochondria exclusively due to its positive charge, re-equilibrates in the cytosol as the mitochondrial membrane potential collapses upon FCCP treatment (Fig. S4C and D). JC-1 and TMRM report a similar time course of FCCP-induced depolarization suggesting that both are reliable reporters of changes in $\Delta\Psi$m at the whole-cell level.

A new combination of probes for ratiometric measurement of $\Delta\Psi$m in oocytes

Our data suggest TMRM has several advantages over JC-1, including its more uniform potentiometric distribution into mitochondria and

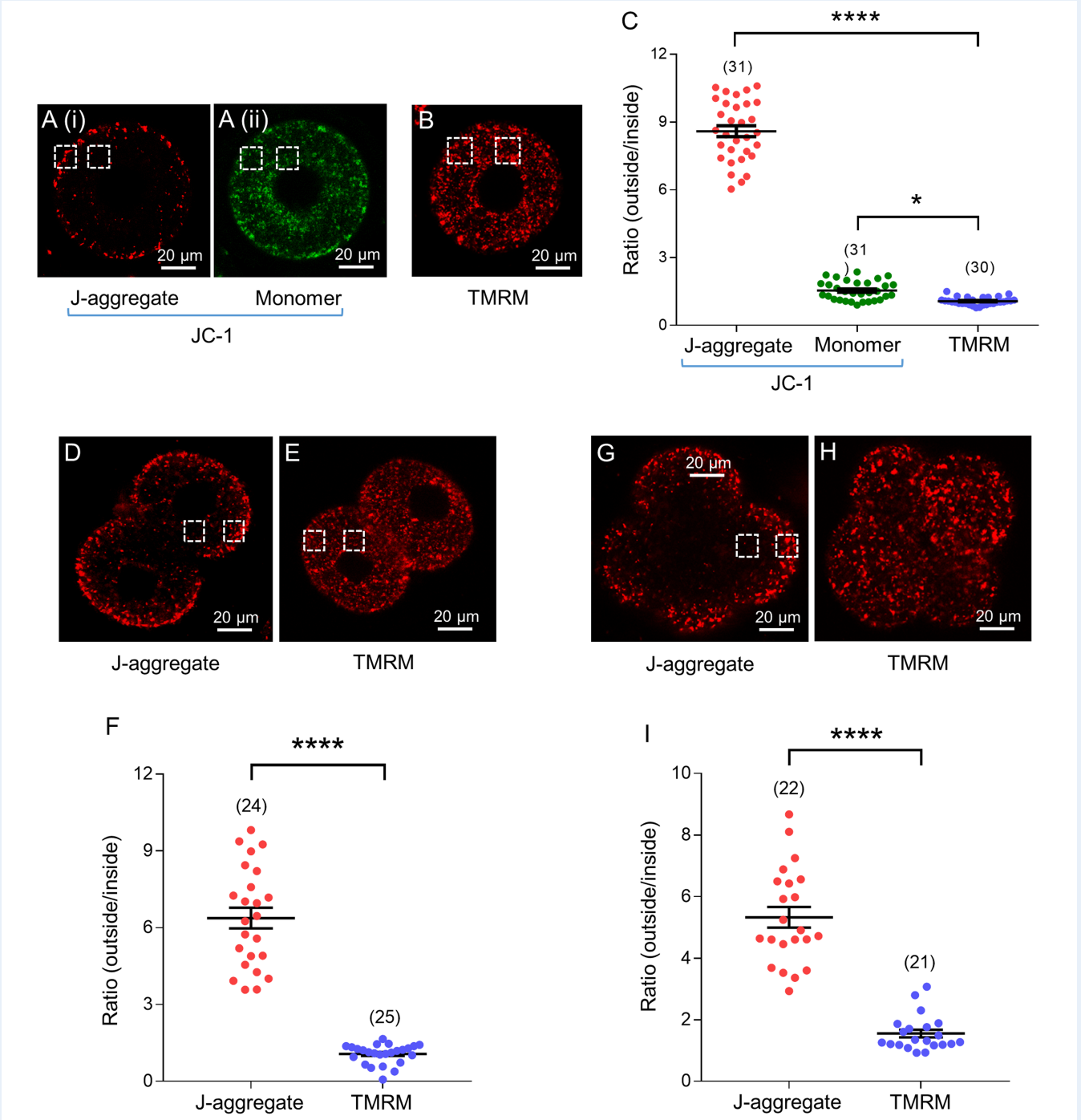

Figure 1 Distribution of JC-1 and TMRM. (**A**) J-aggregate (i) and monomer (ii) distributions after loading with JC-1 (1 μg/ml). (**B**) TMRM (25 nM) fluorescence distribution in GV oocyte. (**C**) Ratio of the fluorescence intensities in cortex and cytoplasm. (**D**) J-aggregate and (**E**) TMRM-labeled 2-cell embryos. (**F**) Ratios of cortex/cytoplasm fluorescence intensities of J-aggregates and TMRM. (**G**) J-aggregate and (**H**) TMRM labeled 4-cell embryos. (**I**) Ratios of cortex/cytoplasm fluorescence intensities of J-aggregates and TMRM. Results are presented from three replicate experiments for each stage. $^{*}P \leq 0.05$, compared to TMRM; $^{****}P \leq 0.0001$, compared to TMRM. Error bars show SE of the mean. *n* = Total number of oocyte/embryos analyzed.

decreased toxicity. The one advantage of JC-1 is that the ΔΨm-sensitive J-aggregate fluorescence can be expressed as a ratio against the fluorescence of the monomer, which in theory provides a measure of mitochondrial activity that is independent of mitochondrial mass. Thus, to take advantage of the properties of TMRM, we have combined it with other mitochondria-targeted fluorescent indicators that are insensitive to ΔΨm (MTG or mito-Dendra); an approach that has been successful in other cell types (Lemasters and Ramshesh, 2007).

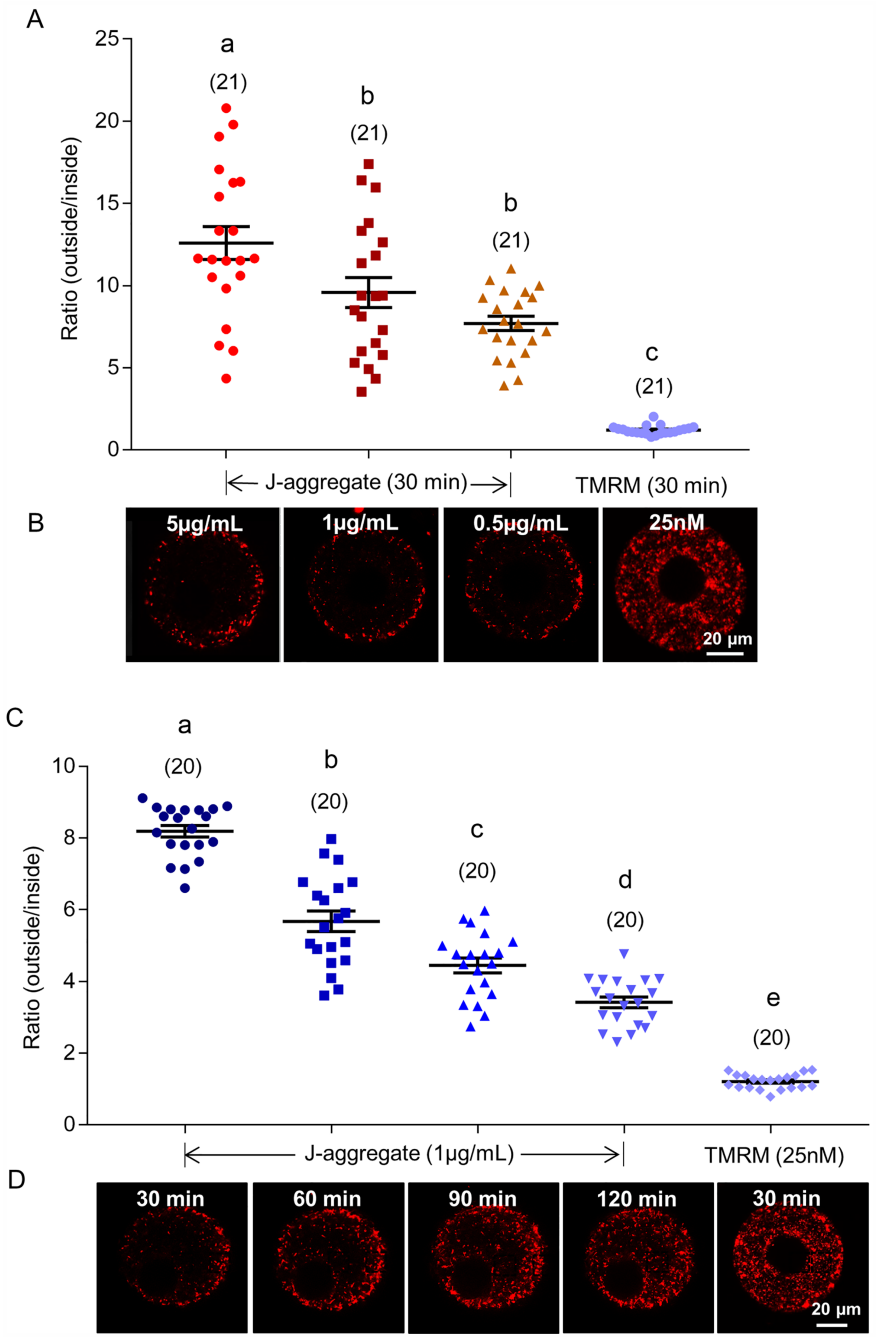

Figure 2 Effect of JC-1 concentration and time on spatial distribution of J-aggregates in oocytes. (**A**) Quantification of spatial distribution of J-aggregates after incubation with various JC-1 concentrations for the same period of time (30 minutes). Oocytes were also cultured in TMRM (25 nM) for 30 minutes. ANOVA was used to compare between groups. A statistical comparison was shown as letters, a versus b represents $P \leq 0.01$; c versus a or b represents $P \leq 0.0001$. (**B**) Representative images of oocytes used for quantification in A. (**C**) Quantification of outside/inside ratios of J-aggregates after incubation for different periods of time in the same concentration of JC-1 (1 μg/ml). For comparison, oocytes were also cultured in TMRM (25 nM) for 30 minutes. A statistical comparison was shown as letters after using ANOVA, all differences between groups were $P \leq 0.0001$ except that comparison between 90 and 120 minutes (c versus d) was $P \leq 0.001$. (**D**) Representative images of oocytes used for quantification in C. Results were combined from 20 oocytes from three replicate experiments. The ratio on the Y-axis was obtained by dividing the fluorescence intensity of the region of interest (ROI) in cortex by that in the cytoplasm. Error bars show SE of the mean.

Oocytes were loaded with TMRM and MTG and imaged using confocal microscopy. Addition of FCCP caused the predicted decrease in TMRM fluorescence, while MTG remained essentially unchanged (Fig. 3A and B). The TMRM/MTG fluorescence ratio can be calculated and provides a means of measuring $\Delta\Psi m$ independent of mitochondrial mass (Fig. 3C).

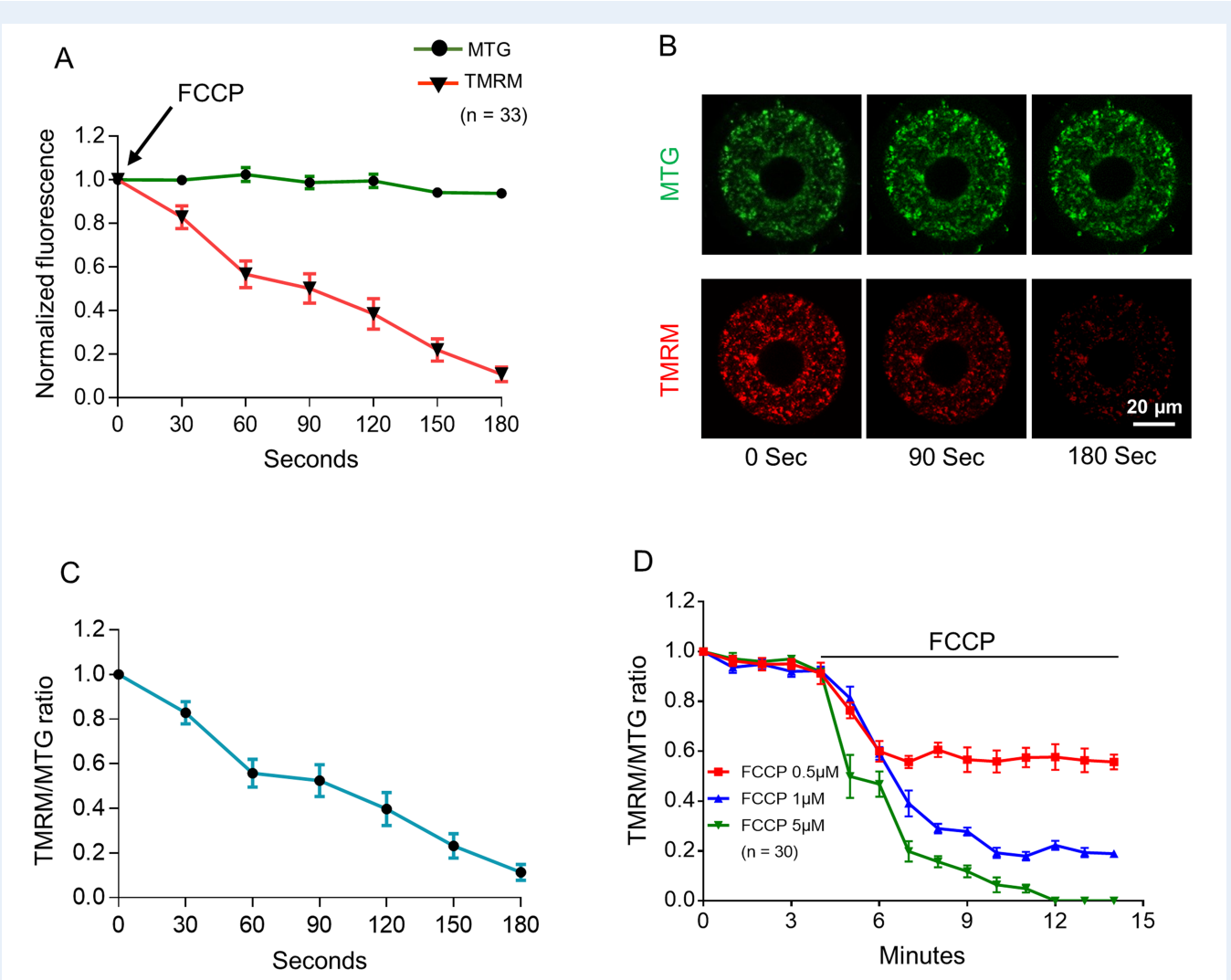

Figure 3 Combination of probes for ratiometric measurement of ΔΨm in oocytes. (**A**) After loading with TMRM and MTG for 30 minutes, loss in fluorescence intensities were monitored. (**B**) Representative images for MTG and TMRM fluorescence. (**C**) TMRM/MTG fluorescence ratio plotted after carbonyl cyanide-p-trifluoromethoxyphenylhydrazone (FCCP) addition. (**D**) Comparison of TMRM/MTG fluorescence over time after addition of different concentrations of FCCP. The experiments were repeated three times each and the values before FCCP addition were normalized to 1. Error bars show SE of the mean.

We next sought to examine whether the TMRM/MTG co-labeling could discriminate between conditions that lead to different resting ΔΨm. Oocytes were loaded with TMRM and MTG as above and a concentration response to FCCP (0.5, 1 and 5 µM) was examined (Fig. 3D). To directly compare the three conditions, the baseline TMRM/MTG ratio was normalized to 1.0 and followed over time (Fig. 3D). The data clearly demonstrate that different concentrations of FCCP lead to different ratios (Fig. 3D), reflecting that this ratiometric measure of mitochondrial activity is sensitive to discrete perturbations in ΔΨm. Thus, this indicator combination can be used to discriminate ΔΨm in different populations of oocytes.

Recording ΔΨm through the duration of oocyte maturation

We next examined whether oocyte maturation is accompanied by any fluctuations in ΔΨm. Given that TMRM equilibrates across the inner mitochondrial membrane according to Nernstian principles, decreases in ΔΨm lead to the loss of TMRM down the potentiometric gradient and increases in ΔΨm result in the accumulation of TMRM. As such, in order to measure any increases in ΔΨm, a low concentration of TMRM (5 nM) was included during imaging.

MTG fluorescence remains constant during the 14 hours of oocyte maturation, while TMRM shows a 50% increase in fluorescence over the period of 100–400 minutes, after which it remains steady (Fig. 4A). The TMRM/MTG ratio shows an increase in ΔΨm during oocyte maturation (Fig. 4A and B). This increase, which starts around the expected time of GVBD, indicates that maturation-dependent changes in ΔΨm may be an important feature of successful oocyte maturation. In support of this, the increase in ΔΨm is dependent on meiotic progression because no excursions in fluorescence or the TMRM/MTG ratio were observed if oocytes were maintained in meiotic arrest for the duration of the recording (Fig. 4C and D).

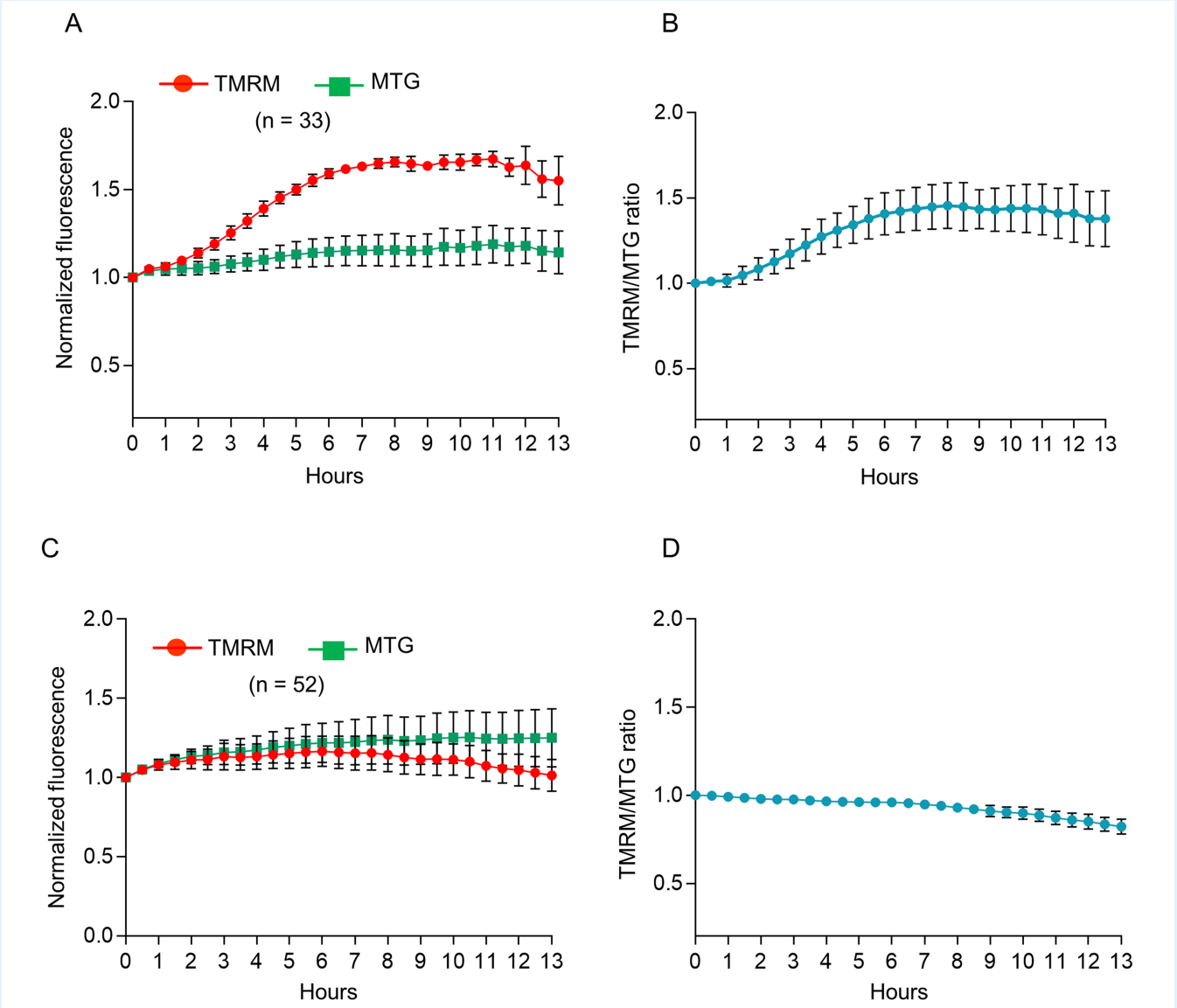

Figure 4 **Increase in ΔΨm during oocyte maturation**. GV oocytes were incubated with TMRM and MTG for 30 minutes and then matured *in vitro* in medium containing low TMRM concentration (5 nM). (**A**) Increase in TMRM fluorescence between 1.5 and 7 hours but with constant levels of MTG fluorescence. (**B**) Increase in TMRM/MTG ratio during oocyte maturation. (**C**) Oocyte meiotic maturation was blocked by adding 200 μM 3-isobutyl-1-methylxanthine (IBMX) to culture medium. This prevented the increase in TMRM fluorescence and the increase in TMRM/MTG fluorescence ratio (**D**). Each experiment was repeated at least three times. Error bars show SE of the mean.

Measuring spatial distribution of ΔΨm

Having shown that long-term recordings of dynamic changes in ΔΨm are feasible in oocytes, we next sought to determine whether combinations of indicators could be reliably used to measure the spatial distribution of ΔΨm within the oocyte. Mito-Dendra expressing oocytes from *PhAM*$^{loxP/loxP}$; *Gdf9Cre* mice were loaded with TMRM as above and confocal imaging was performed to obtain high-resolution images at both wavelengths. The images were arithmetically divided pixel × pixel to provide a ratiometric image of ΔΨm independent of concentration of mitochondria in different locations across the oocyte. It is clear from examining the ratio images that, consistent with TMRM distribution, there is no evidence of a peri-cortical increase in ΔΨm in oocytes at different stages of maturation. In fact, at the GV stage, peri-nuclear mitochondria (within 5 μM of GV, see Fig. S5A) show a small but significant increase in ΔΨm compared to the rest of the mitochondria (Fig. 5A–D). Further analysis revealed that at metaphase I, there was a significant 20% difference in ΔΨm across the oocyte; spindle-associated mitochondria had higher ΔΨm than non-spindle associated mitochondria (Fig. 5E–H, and S5B). Subcellular heterogeneity was also observed in MII stage oocytes (Fig. 5I–L and S5C), although less obvious than that seen at MI. In MII stage oocytes, we compared ΔΨm in the upper portion of the spindle-

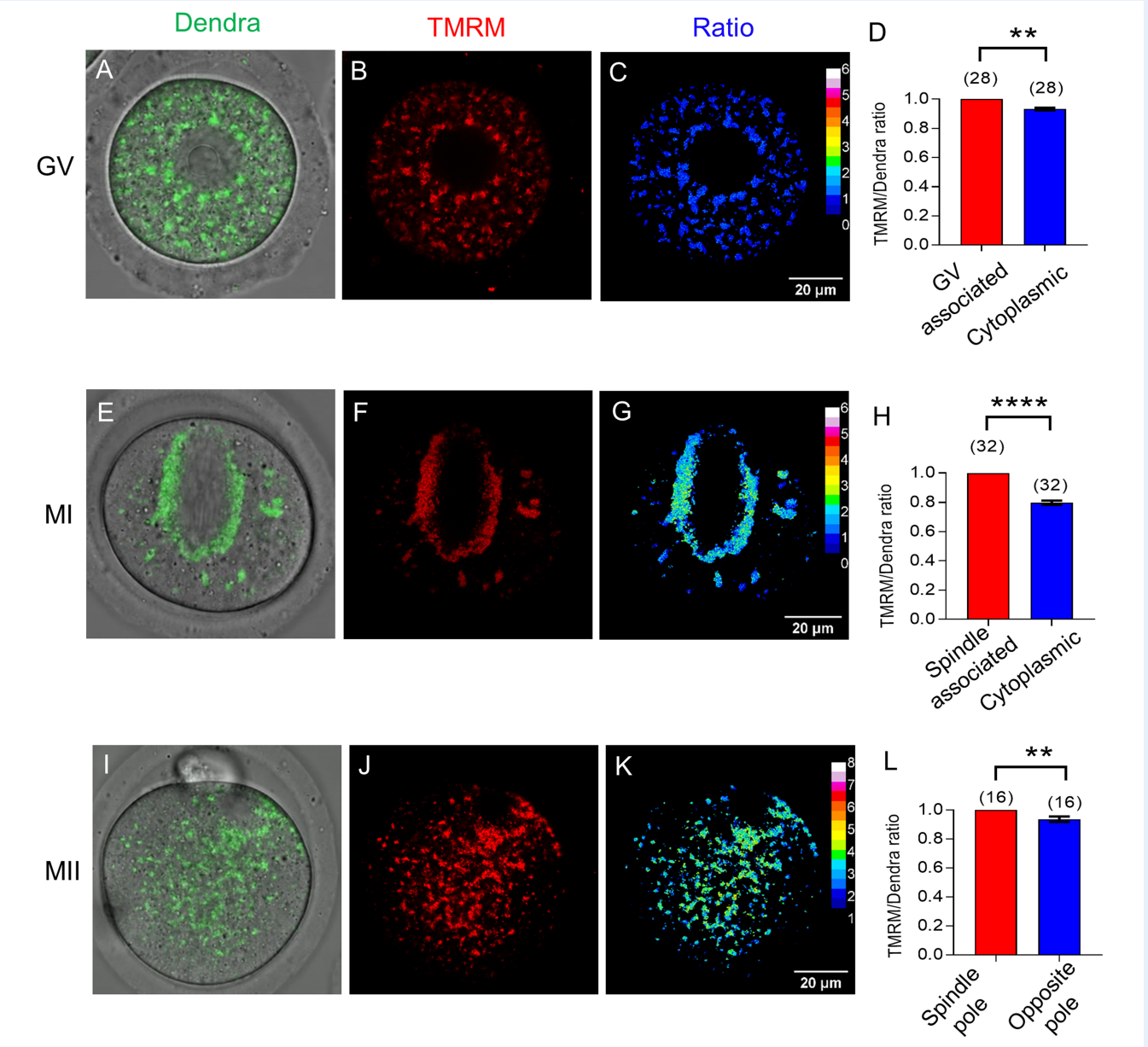

Figure 5 Spatial distribution of ΔΨm during oocyte maturation. Mito-Dendra expressing oocytes from *PhAM*$^{loxP/loxP}$; *Gdf9Cre* mice at GV, metaphase I and II (MI and MII) were loaded with TMRM. High-resolution confocal images were obtained at both wavelengths to calculate TMRM/Dendra ratios across various regions of the oocytes. (**A**–**D**) Mitochondria around the GV have higher membrane potential than the mitochondria not surrounding the GV. $n = 28$. ****, $P < 0.01$. (**E**–**H**) GV oocytes were cultured *in vitro* for 8 hours to obtain MI oocytes. MI oocytes show higher ΔΨm in mitochondria associated with spindle than in those away from the spindle. $n = 32$. ****, $P < 0.0001$. (**I**–**L**) Ovulated MII oocytes were collected 14 hours after hCG injection. Mitochondria around the MII spindle (spindle pole) have higher ΔΨm than those at opposite pole. $n = 16$. **, $P < 0.01$. Data shown as mean ± SEM.

containing hemisphere with that at the opposite pole of the oocyte and found that ΔΨm was approximately 7% higher in the spindle region (Fig. 5L). To determine whether mitochondrial cluster size might have caused differences in ΔΨm, we correlated ΔΨm with mitochondrial cluster sizes in MI stage oocytes. The results show that ΔΨm did not correlate with mitochondrial cluster size (Fig. S6). Thus, at each stage of oocyte maturation, mitochondrial activity is highest in the peri-nuclear region.

Discussion

Mitochondrial function is critical to oocyte quality. Conditions that cause sub-fertility such as maternal ageing, obesity and metabolic disease are widely regarded to be acting through compromising mitochondrial activity, causing reduced ATP and increased ROS (Grindler and Moley, 2013; Schatten *et al.*, 2014; Wu *et al.*, 2015). The growing appreciation of mitochondrial function in oocyte and embryo devel-

opment compelled us to investigate $\Delta\Psi$m in oocytes with a particular focus on the spatial distribution of $\Delta\Psi$m in the oocyte cytoplasm.

To tackle this question, it was first necessary to investigate the properties of the fluorescent indicators used for measuring $\Delta\Psi$m. The discordance in the literature regarding sub-cellular heterogeneity in $\Delta\Psi$m was confirmed in our investigations in that JC-1 and TMRM report very different distributions in $\Delta\Psi$m in mouse oocytes and early embryos. JC-1 showed high $\Delta\Psi$m in the oocyte cortex relative to the inner cytoplasm, similar to previously reported patterns (Van Blerkom *et al.*, 2000, 2002, 2003, 2008; Van Blerkom and Davis, 2006; Tatone *et al.*, 2011; Zhao *et al.*, 2011; Boudoures *et al.*, 2017; Pasquariello *et al.*, 2019), while in contrast, TMRM distribution showed a homogeneous $\Delta\Psi$m distribution across the cytoplasm (Dumollard *et al.*, 2004; Zhang *et al.*, 2006; Igosheva *et al.*, 2010). Despite efforts to adjust concentration and equilibration times, the J-aggregate distribution remained higher in the cortex. The ability of longer incubation times to reduce the gradient of J-aggregate across the oocyte indicates that diffusion and membrane permeability properties, combined with a non-linear J-aggregate formation, may contribute to the high levels of J-aggregate fluorescence in the cortical mitochondria. Nevertheless, while challenging to use for subcellular distribution, the relative level of red/green fluorescence at the whole cell level, is sensitive to membrane potential collapse so can be used to report overall differences in $\Delta\Psi$m between groups of oocytes.

TMRM is conceptually a more predictable indicator to work with, as it is small and highly permeable and is predicted to distribute across membranes according to Nernstian principles (Nicholls and Ward, 2000). As such, it is reasonable to conclude that the failure of TMRM to report an increase $\Delta\Psi$m in the cortex indicates $\Delta\Psi$m is more homogeneously distributed in the oocyte cytoplasm. In addition, its lack of toxicity makes it ideal for long-term imaging experiments and it can also be used ratiometrically by combining with a second spectrally separable mitochondrial reporter that is insensitive to $\Delta\Psi$m. This approach provides a reliable method for use of TMRM to measure $\Delta\Psi$ independent of mitochondrial mass.

We have found MTG, or mitochondria-targeted GFP/Dendra, to be reliable reporters for combining with TMRM in oocytes. While both work well, we find that mitochondrially targeted fluorescent proteins provide a cleaner signal than MTG, which can also bind to non-mitochondrial sites in the cytoplasm. Similar ratiometric approaches have been used in a variety of other cell types (Pendergrass *et al.*, 2004; Lemasters and Ramshesh, 2007; Mourier *et al.*, 2015). One important caveat with this approach is that the behavior of the second reporter must solely report mitochondrial mass, and not be influenced by the physiological state of the oocyte or the location of mitochondria in the cell. Careful consideration of these issues is needed for every experimental condition.

We have taken advantage of this ratiometric approach to undertake the first recordings of $\Delta\Psi$m during the entire time course of oocyte maturation. Interestingly, the increased $\Delta\Psi$m we observe during oocyte maturation shows good temporal correlation with the previously reported increase in ATP during oocyte maturation (Yu *et al.*, 2010; Dalton *et al.*, 2014). Oocytes that remain arrested at the GV stage throughout the entire recording period show no excursions in $\Delta\Psi$m or ATP. This indicates that on progression into meiosis, the energy demands increase causing an adaptive response that drives an increase in $\Delta\Psi$m to provide the ATP necessary to drive the events of maturation.

The ability to perform arithmetic ratiometric image analysis of the TMRM/mito-Dendra couplet has allowed us to further interrogate the spatial distribution of $\Delta\Psi$m across the oocyte. Our results provide no evidence for a peri-cortical increase in $\Delta\Psi$m, but do reveal other heterogeneities may exist. At the GV and MII stages, modest increases (<10%) in $\Delta\Psi$m were observed in the region of the GV and MII spindle. These differences, while statistically significant, are small and as such, the physiological relevance needs further investigation. One potential function of polarized mitochondria in the peri-nuclear region is the provision of ATP to fuel nuclear transport, while at the MII stage, they may serve to maintain function of the arrested but highly dynamic MII spindle (Nakagawa and FitzHarris, 2017; Zhang *et al.*, 2017).

The most dramatic compartmentalization of $\Delta\Psi$m was apparent in the spindle-associated mitochondria at the MI stage. Mitochondria in this region showed a ratio increase of around 25% compared to peripheral mitochondria. Like the local $\Delta\Psi$m increases seen in regions of GV and MII stage oocytes, it is tempting to speculate the local increase in $\Delta\Psi$m at the MI stage reflects an adaptive response to the increased metabolic demands of spindle formation and function during this critical phase of oocyte maturation. While recent studies in neurons predict mitochondrial localization can influence spatial gradients of ATP that play a role in localized translation (Cioni *et al.*, 2019), it is unknown at this stage whether highly active mitochondria close to the MI spindle provide any advantage to spindle formation or fidelity.

How $\Delta\Psi$m can be locally regulated also needs further investigation. Response to a local high rate of ATP consumption may be one possibility, but it may also reflect the mitochondrial organization in relation to the ER. In mouse oocytes, the ER is known to surround the MI spindle (FitzHarris *et al.*, 2007; Dalton and Carroll, 2013) and local Ca^{2+} cycling between the ER-cytosol-mitochondria has been reported to influence mitochondrial function (Mak *et al.*, 1999). Alternatively, if dynein-mediated mitochondrial trafficking favored those mitochondria with a higher $\Delta\Psi$m, more highly polarized mitochondria would accumulate in the spindle region.

In summary, our data show that there is a maturation-dependent increase in $\Delta\Psi$m and that mitochondria in the vicinity of the first meiotic spindle show a local increase in $\Delta\Psi$m. We find no evidence for the previously reported sub-cortical increase in $\Delta\Psi$m and suggest that these observations are a reflection of the behavior of the indicator, JC-1, rather than mitochondria. Our findings suggest that mitochondrial activity shows both temporal and spatial regulation during the process of mouse oocyte maturation in vitro.

Supplementary data

Supplementary data are available at *Molecular Human Reproduction* online.

Acknowledgements

The authors would like to thank Monash Micro Imaging for support with confocal imaging and Gyuri Szbadkai (UCL) for advice on ratiometric image analysis.

Author's roles

All authors qualify for authorship by contributing substantially to this article. UAZ, DA and JC developed the original concept of this study collectively. Data collection was performed by UAZ, JL, OC and DA., statistical analysis by UAZ. RLR contributed to the discussion and interpretation of the results and writing the manuscript. All authors have contributed to critical discussion, reviewed the final version of the article and approved it for publication.

Funding

The authors would like to acknowledge the financial support from National Health and Medical Research Council and Australian Research Council, Australia. Additionally, U.A.Z. was supported by the Iraqi Higher Education and Scientific Research Ministry Ph.D. scholarship and O.C. by TUBITAK-1059B191601275.

Conflict of interest

There are no competing interests related to this study.

References

Ben-Meir A, Burstein E, Borrego-Alvarez A, Chong J, Wong E, Yavorska T, Naranian T, Chi M, Wang Y, Bentov Y *et al.* Coenzyme Q10 restores oocyte mitochondrial function and fertility during reproductive aging. *Aging Cell* 2015;**14**:887–895.

Boots CE, Boudoures A, Zhang W, Drury A, Moley KH. Obesity-induced oocyte mitochondrial defects are partially prevented and rescued by supplementation with co-enzyme Q10 in a mouse model. *Hum Reprod* 2016;**31**:2090–2097.

Boudoures AL, Saben J, Drury A, Scheaffer S, Modi Z, Zhang W, Moley KH. Obesity-exposed oocytes accumulate and transmit damaged mitochondria due to an inability to activate mitophagy. *Dev Biol* 2017;**426**:126–138.

Cioni JM, Lin JQ, Holtermann AV, Koppers M, Jakobs MAH, Azizi A, Turner-Bridger B, Shigeoka T, Franze K, Harris WA *et al.* Late endosomes act as mRNA translation platforms and sustain mitochondria in axons. *Cell* 2019;**176**:56–72.e15.

Dalton CM, Carroll J. Biased inheritance of mitochondria during asymmetric cell division in the mouse oocyte. *J Cell Sci* 2013;**126**:2955–2964.

Dalton CM, Szabadkai G, Carroll J. Measurement of ATP in single oocytes: impact of maturation and cumulus cells on levels and consumption. *J Cell Physiol* 2014;**229**:353–361.

Dumollard R, Marangos P, Fitzharris G, Swann K, Duchen M, Carroll J. Sperm-triggered [Ca^{2+}] oscillations and Ca^{2+} homeostasis in the mouse egg have an absolute requirement for mitochondrial ATP production. *Development* 2004;**131**:3057–3067.

Eichenlaub-Ritter U, Vogt E, Yin H, Gosden R. Spindles, mitochondria and redox potential in ageing oocytes. *Reprod Biomed Online* 2004;**8**:45–58.

FitzHarris G, Marangos P, Carroll J. Changes in endoplasmic reticulum structure during mouse oocyte maturation are controlled by the cytoskeleton and cytoplasmic dynein. *Dev Biol* 2007;**305**:133–144.

Grindler NM, Moley KH. Maternal obesity, infertility and mitochondrial dysfunction: potential mechanisms emerging from mouse model systems. *MHR: basic science of reproductive. Medicine* 2013;**19**:486–494.

Igosheva N, Abramov AY, Poston L, Eckert JJ, Fleming TP, Duchen MR, McConnell J. Maternal diet-induced obesity alters mitochondrial activity and redox status in mouse oocytes and zygotes. *PloS One* 2010;**5**:e10074.

Lan ZJ, Xu X, Cooney AJ. Differential oocyte-specific expression of Cre recombinase activity in GDF-9-iCre, Zp3cre and Msx2Cre transgenic mice. *Biol Reprod* 2004;**71**:1469–1474.

Lemasters JJ, Ramshesh VK. Imaging of mitochondrial polarization and depolarization with cationic fluorophores. *Methods Cell Biol* 2007;**80**:283–295.

Mak DO, McBride S, Foskett JK. ATP regulation of type I inositol 1,4,5-trisphosphate receptor channel gating by allosteric tuning of Ca(2+) activation. *J Biol Chem* 1999;**274**:22231–22237.

Mitchell P, Moyle J. Chemiosmotic hypothesis of oxidative phosphorylation. *Nature* 1967;**213**:137–139.

Mourier A, Motori E, Brandt T, Lagouge M, Atanassov I, Galinier A, Rappl G, Brodesser S, Hultenby K, Dieterich C *et al.* Mitofusin 2 is required to maintain mitochondrial coenzyme Q levels. *J Cell Biol* 2015;**208**:429–442.

Nakagawa S, FitzHarris G. Intrinsically defective microtubule dynamics contribute to age-related chromosome segregation errors in mouse oocyte meiosis-I. *Curr Biol* 2017;**27**:1040–1047.

Nicholls DG, Ward MW. Mitochondrial membrane potential and neuronal glutamate excitotoxicity: mortality and millivolts. *Trends Neurosci* 2000;**23**:166–174.

Ottosen LD, Hindkjaer J, Ingerslev J. Light exposure of the ovum and preimplantation embryo during ART procedures. *J Assist Reprod Genet* 2007;**24**:99–103.

Pasquariello R, Ermisch AF, Silva E, McCormick S, Logsdon D, Barfield JP, Schoolcraft WB, Krisher RL. Alterations in oocyte mitochondrial number and function are related to spindle defects and occur with maternal aging in mice and humansdagger. *Biol Reprod* 2019;**100**:971–981.

Pendergrass W, Wolf N, Poot M. Efficacy of MitoTracker green and CMXrosamine to measure changes in mitochondrial membrane potentials in living cells and tissues. *Cytometry A* 2004;**61**:162–169.

Pham AH, McCaffery JM, Chan DC. Mouse lines with photo-activatable mitochondria to study mitochondrial dynamics. *Genesis (New York)* 2000;**2012**:833–843.

Schatten H, Sun Q-Y, Prather R. The impact of mitochondrial function/dysfunction on IVF and new treatment possibilities for infertility. *Reprod Biol Endocrinol* 2014;**12**:111.

Tatone C, Heizenrieder T, Di Emidio G, Treffon P, Amicarelli F, Seidel T, Eichenlaub-Ritter U. Evidence that carbonyl stress by methylglyoxal exposure induces DNA damage and spindle aberrations, affects mitochondrial integrity in mammalian oocytes and contributes to oocyte ageing. *Hum Reprod (Oxford, England)* 2011;**26**:1843–1859.

Tilly JL, Sinclair DA. Germline energetics, aging, and female infertility. *Cell Metab* 2013;**17**:838–850.

Van Blerkom J, Davis P. High-polarized ($\Delta\Psi$m HIGH) mitochondria are spatially polarized in human oocytes and early embryos in stable subplasmalemmal domains: developmental significance and the

concept of vanguard mitochondria. *Reprod Biomed Online* 2006;**13**: 246–254.

Van Blerkom J, Davis P. Mitochondrial signaling and fertilization. *MHR*: basic science of reproductive. *Medicine* 2007;**13**:759–770.

Van Blerkom J, Davis P, Alexander S. Differential mitochondrial distribution in human pronuclear embryos leads to disproportionate inheritance between blastomeres: relationship to microtubular organization, ATP content and competence. *Hum Reprod* 2000;**15**:2621–2633.

Van Blerkom J, Davis P, Alexander S. Inner mitochondrial membrane potential ($\Delta\Psi$m), cytoplasmic ATP content and free Ca^{2+} levels in metaphase II mouse oocytes. *Hum Reprod* 2003;**18**: 2429–2440.

Van Blerkom J, Davis P, Mathwig V, Alexander S. Domains of high-polarized and low-polarized mitochondria may occur in mouse and human oocytes and early embryos. *Hum Reprod* 2002;**17**: 393–406.

Van Blerkom J, Davis P, Thalhammer V. Regulation of mitochondrial polarity in mouse and human oocytes: the influence of cumulus derived nitric oxide. *Mol Hum Reprod* 2008;**14**:431–444.

Van Blerkom J, Runner MN. Mitochondrial reorganization during resumption of arrested meiosis in the mouse oocyte. *Am J Anat* 1984;**171**:335–355.

Wang Q, Ratchford AM, Chi MM, Schoeller E, Frolova A, Schedl T, Moley KH. Maternal diabetes causes mitochondrial dysfunction and meiotic defects in murine oocytes. *Mol Endocrinol (Baltimore, Md)* 2009;**23**:1603–1612.

Wu LL, Russell DL, Wong SL, Chen M, Tsai TS, St John JC, Norman RJ, Febbraio MA, Carroll J, Robker RL. Mitochondrial dysfunction in oocytes of obese mothers: transmission to offspring and reversal by pharmacological endoplasmic reticulum stress inhibitors. *Development* 2015;**142**:681–691.

Yu Y, Dumollard R, Rossbach A, Lai FA, Swann K. Redistribution of mitochondria leads to bursts of ATP production during spontaneous mouse oocyte maturation. *J Cell Physiol* 2010;**224**: 672–680.

Zhang QH, Yuen WS, Adhikari D, Flegg JA, FitzHarris G, Conti M, Sicinski P, Nabti I, Marangos P, Carroll J. Cyclin A2 modulates kinetochore-microtubule attachment in meiosis II. *J Cell Biol* 2017;**216**:3133–3143.

Zhang X, Wu XQ, Lu S, Guo YL, Ma X. Deficit of mitochondria-derived ATP during oxidative stress impairs mouse MII oocyte spindles. *Cell Res* 2006;**16**:841.

Zhao XM, Du WH, Wang D, Hao HS, Liu Y, Qin T, Zhu HB. Effect of cyclosporine pretreatment on mitochondrial function in vitrified bovine mature oocytes. *Fertil Steril* 2011;**95**:2786–2788.